Hexagonal GaN grown on GaAs{11n} substrates by metalorganic vapor-phase epitaxy using AlAs intermediate layers

AUTHOR(S):

Funato, M; Yamamoto, S; Kaisei, K; Shimogami, K; Fujita, S; Fujita, S

CITATION:

Funato, M ...[et al]. Hexagonal GaN grown on GaAs{11n} substrates by metalorganic vapor-phase epitaxy using AlAs intermediate layers. APPLIED PHYSICS LETTERS 2001, 79(25): 4133-4135

ISSUE DATE:

2001-12-17

URL:

http://hdl.handle.net/2433/39647

Hexagonal GaN grown on GaAs{11*n*} substrates by metalorganic vapor-phase epitaxy using AlAs intermediate layers

Mitsuru Funato,[a] Shuichiro Yamamoto, Kiyohiro Kaisei, Koichiro Shimogami, Shizuo Fujita, and Shigeo Fujita
Department of Electronic Science and Engineering, Kyoto University, Kyoto 606-8501, Japan

(Received 22 May 2001; accepted for publication 9 October 2001)

Hexagonal GaN (*h*-GaN) layers are grown by metalorganic vapor-phase epitaxy on GaAs{11*n*}A and B ($n=8, 4, 3, 2, 1$) substrates using AlAs intermediate layers. The best quality of *h*-GaN is obtained on $(1\bar{1}4)$B, where the crystallographic relationship is found from a pole figure to be *h*-GaN{0001}‖GaAs$(3\bar{3}5)$B and *h*-GaN$\{10\bar{1}2\}$‖GaAs(001). We propose a simple model that explains why such a crystallographic relationship is easily realized on {114} resulting in the superior structural and optical properties. Furthermore, from a comparison between the growth on the A and B substrates, it is pointed out that the polarity is a key factor in determining the crystallographic properties. © *2001 American Institute of Physics.* [DOI: 10.1063/1.1426275]

GaN grown on sapphire substrates has already made a significant technological impact on optoelectronics.[1] However, sapphire is not suitable for device processes such as etching, cleaving, and forming electrodes, which motivates the study on alternative substrates. In particular, Si, SiC, and GaAs have received an increasing interest due to larger wafer size, higher conductivity, and advanced technology of these substrates.[2–6] Among them, the GaAs substrate is quite attractive because the mismatch in the thermal expansion coefficients is the smallest [$\sim$1.8% for GaN(0001)], and the integration of GaN with GaAs-based devices might be possible.

According to the standard framework,[4–6] cubic GaN (*c*-GaN) is grown on GaAs(001) substrates, and hexagonal GaN (*h*-GaN) is grown on GaAs{111} substrates. This is quite natural from the viewpoint of the crystalline structures. On the contrary, we have recently demonstrated that single-phase *h*-GaN can be grown even on GaAs(001) if an AlAs layer is grown in between.[7–9] This result allows us to grow *h*-GaN not only on {111} but also on a series of {11*n*} substrates, and to find the optimum orientation for higher quality of *h*-GaN epilayers. Based on this, in this study, *h*-GaN layers are grown on GaAs{11*n*}A and B substrates ($n=8, 4, 3, 2, 1$) and their properties are characterized. We show that the $(1\bar{1}4)$B substrate[10] is superior to the others and discuss what causes this experimental result.

The samples were grown by atmospheric-pressure metalorganic vapor-phase epitaxy (MOVPE). The growth was carried out on the A and B substrates simultaneously. An AlAs intermediate layer ($\leqslant$20 nm) was first grown at 700 °C using trimethylaluminum and tertiarybutylarsine as source precursors. Then, the GaN layer was grown at 650 °C using triethylgallium and dimethylhydrazine. The molar flow ratio (V/III) was 100, which is an optimized value for *h*-GaN on AlAs/GaAs(001). The growth rate was about 300 nm h^{-1}, and the film thickness was 300 nm. The crystallographic properties were examined by x-ray diffraction (XRD) using Cu $K\alpha_1$ radiation as an x-ray source. In particular, pole figures were investigated in detail to elucidate the crystalline structure and orientation of the grown films.

Before showing the results on *h*-GaN-on-AlAs/GaAs, the results on the direct growth of GaN on GaAs{11*n*} are briefly summarized. The pole figure measurements showed that the grown films are made up of a mixture of the cubic and hexagonal phases, irrespective of the substrate orientation and polarity. For the cubic phase, the crystallographic relationship was *c*-GaN(001)‖GaAs(001), while for the hexagonal phase, that was *h*-GaN{0001}‖GaAs{111}. These relationships are understandable within the standard framework.[4–6] It should be noted that even on the GaAs{111}A and B substrates, GaN grown under the present growth conditions included the cubic phase, similar to the result by Sasaki *et al.*[5] On the other hand, as will be shown next, when an AlAs layer was inserted between GaN and GaAs, *c*-GaN was not detected on any substrates. From these results, it is clear that AlAs promotes the growth of the hexagonal phase, and therefore we always use AlAs as an intermediate layer in the rest of this study.

Firstly, we show the results on GaN grown on AlAs/GaAs$(11n)$B. Figure 1 depicts an example of the XRD pole figure measurements. The substrate is $(1\bar{1}4)$B in this particular case. In Fig. 1, χ refers to the angle between the GaAs surface and the plane under measurement. The diffractions from the *h*-GaN{0002} (which is equivalent to *c*-GaN{111}), *h*-GaN$\{10\bar{1}2\}$, and GaAs{335} planes were measured. Since the lattice parameter of AlAs agrees quite well with that of GaAs, AlAs diffraction spots are always included in GaAs diffraction spots (but the contribution is trivial due to the thickness). As shown in Fig. 1, the six-fold *h*-GaN$\{10\bar{1}2\}$ diffractions were detected. At the center of these six diffraction spots, *h*-GaN{0002} and/or *c*-GaN{111} diffraction can be seen. If this diffraction is due to *c*-GaN{111}, however, three other {111} diffractions should be observed because there are four equivalent *c*-GaN{111} planes in principle. Therefore, we infer that the detected diffraction is derived from *h*-GaN{0002} and that the grown film is single-phase *h*-GaN. In order to extract the crystallographic relationship between *h*-GaN and the GaAs$(1\bar{1}4)$B substrate, we have to note that the

[a]Electronic mail: funato@kuee.kyoto-u.ac.jp

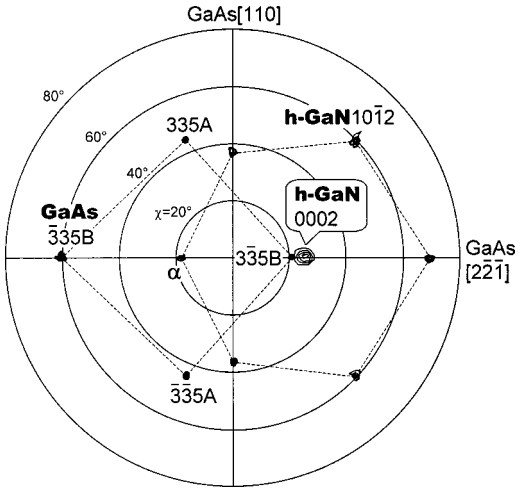

FIG. 1. Pole figure of GaN/AlAs/GaAs(1$\bar{1}$4)B. The diffractions from the *h*-GaN{0002}, *h*-GaN{10$\bar{1}$2}, and GaAs{335} planes are shown together. Isointensity contour levels at 4^m ($m=0,1,2,3,\cdots$) cps.

h-GaN{0002} diffraction spot almost overlaps with the GaAs($\bar{3}\bar{3}$5)B spot, and that one of the *h*-GaN{10$\bar{1}$2} iffraction spots (designated by "α" in Fig. 1) is located at the center of four-fold GaAs{335} diffraction spots. From these findings, it is concluded that the crystallographic relationship is *h*-GaN{0001}‖GaAs($\bar{3}\bar{3}$5)B and *h*-GaN{10$\bar{1}$2}‖GaAs(001). It is worth noting that this relationship involves *h*-GaN{11$\bar{2}$0}‖GaAs(110) as well. These planes are cleavable, and therefore, the cleavability of GaAs is still usable in the present samples.

Why was the above relationship realized between *h*-GaN and AlAs/GaAs? To answer this question, it is interesting to compare the layer spacings, *d*; those are $d_{h\text{-GaN}\{0001\}}=5.185$ Å, $d_{\text{AlAs}\{335\}}=0.8633$ Å, $d_{h\text{-GaN}\{10\bar{1}2\}}=1.890$ Å, and $d_{\text{AlAs}(001)}=5.6611$ Å. $d_{h\text{-GaN}\{0001\}}$ divided by 6 is almost equal to $d_{\text{AlAs}\{335\}}$ and $d_{h\text{-GaN}\{10\bar{1}2\}}$ multiplied by 3 agrees well with $d_{\text{AlAs}(001)}$. We consider that this good "lattice matching" causes the observed crystallographic relationship of *h*-GaN{0001}‖GaAs($\bar{3}\bar{3}$5)B and *h*-GaN{10$\bar{1}$2}‖GaAs(001). The result of the pole figure measurement and this analysis is schematically illustrated in Fig. 2, where the GaAs(1$\bar{1}$0)‖*h*-GaN{11$\bar{2}$0} cross section is viewed along the GaAs[110] direction. The angle formed between *h*-GaN{0001} and *h*-GaN{10$\bar{1}$2} does not perfectly

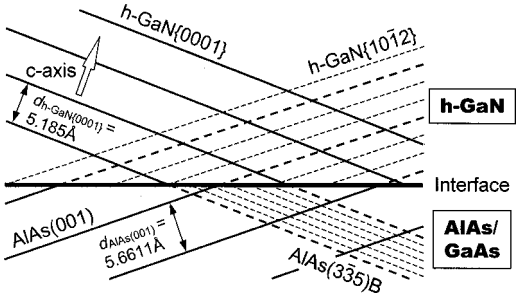

FIG. 2. Schematic of the crystallographic relationship. The GaAs(1$\bar{1}$0)‖*h*-GaN{11$\bar{2}$0} cross section is shown. The solid and broken lines in the *h*-GaN region are *h*-GaN{0001} and {10$\bar{1}$2} planes, respectively. Those in the AlAs region are AlAs(001) and ($\bar{3}\bar{3}$5)B planes, respectively. The thick lines indicate agreement between the layer spacing in *h*-GaN and in AlAs.

TABLE I. Summary on the crystallographic relationship between *h*-GaN and GaAs(11$\bar{n}$)B substrates revealed by the pole figure measurements.

Substrate	Orientation
(1$\bar{1}$8)B	GaN{0001}‖GaAs($\bar{3}\bar{3}$5)B, GaN{10$\bar{1}$2}‖GaAs(001)
(1$\bar{1}$4)B	GaN{0001}‖GaAs($\bar{3}\bar{3}$5)B, GaN{10$\bar{1}$2}‖GaAs(001)
(1$\bar{1}$3)B	GaN{0001}‖GaAs($\bar{3}\bar{3}$5)B, GaN{10$\bar{1}$2}‖GaAs(001)
(1$\bar{1}$2)B	GaN{0001}‖GaAs(1$\bar{1}$1)
(1$\bar{1}$1)B	GaN{0001}‖GaAs(1$\bar{1}$1)

agree with that between GaAs($\bar{3}\bar{3}$5)B and GaAs(001). Due to this small angular difference about 2.9°, the *h*-GaN{0002} spot does not exactly overlap with the GaAs($\bar{3}\bar{3}$5)B in the pole figure shown in Fig. 1.

The XRD pole figure measurements were performed also with other samples grown on GaAs(11*n*)B. Table I is a summary. From Table I, it is found that the crystallographic relationship is categorized into two types; (I) on GaAs(1$\bar{1}$8)B, (1$\bar{1}$4)B, and (1$\bar{1}$3)B, and (II) on GaAs(1$\bar{1}$2)B and (1$\bar{1}$1)B, which are, respectively, called category I and II hereafter. A cause of this will be discussed below.

The crystallinity of the samples grown on GaAs(11$\bar{n}$)B was evaluated in terms of a full width at half maximum (FWHM) of XRD ω scan. For this, the *h*-GaN{0002} planes were measured under a symmetric configuration,[11] which makes fair comparison between the samples possible. The results are shown in Fig. 3(a), where the horizontal axis is the angle between GaAs(001) and the substrate surface. For a comparison, the result for *h*-GaN/AlAs/GaAs(001) is also shown. It is clearly seen that FWHM of GaN on GaAs(1$\bar{1}$4)B is the narrowest as 55 arcmin.

Let us discuss the cause of the results shown in Table I and Fig. 3(a), using Fig. 3(b). In category II [*h*-GaN{0001}‖GaAs(1$\bar{1}$1)], the growth is a simple epitaxy as *c*-{111} is equivalent to *h*-{0002}. Therefore, category II is realized more easily when the substrate surface approaches GaAs(1$\bar{1}$1), in other words, when the density, which is defined as the number of the planes intersecting with the substrate surface per unit length, of GaAs(1$\bar{1}$1) becomes smaller. If we consider this condition for category I, the GaAs(1$\bar{1}$1) density should be larger to suppress *h*-GaN{0001}‖GaAs(1$\bar{1}$1). At the same time,

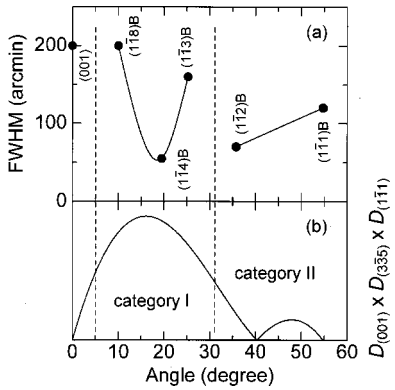

FIG. 3. (a) FHWM of *h*-GaN{0002} diffraction measured by XRD symmetric ω scan. Variation due to the substrate orientation is compared. (b) Calculated product of the densities of GaAs(001), ($\bar{3}\bar{3}$5), and (1$\bar{1}$1) planes. *D* stands for the density of the indicated plane.

h-GaN{0001}‖GaAs(3$\bar{3}$5)B and h-GaN{10$\bar{1}$2}‖GaAs(001) are satisfied in category I. In order to express these conditions numerically, we assumed the probability of the appearance of category I is related to the product of the densities of GaAs(001), (3$\bar{3}$5)B, and (1$\bar{1}$1)B planes. Figure 3(b) shows the calculated result of this product of the densities. Comparing Figs. 3(a) and 3(b), it is found that category I is realized when the product of the densities is larger than a certain value, and that, in category I, a larger value of the product, that is, a higher probability of being category I, causes a better crystalline quality. This good agreement between the experiment and the calculation supports the hypothesis that a driving force in determining the crystalline orientation is related to the densities of the GaAs(001), (3$\bar{3}$5)B, and (1$\bar{1}$1)B on the substrate surface.

For GaN on AlAs/GaAs(11n)A, the crystallographic properties were similarly characterized by the pole figure measurements. For n=8, 4, and 3, it was found that the diffraction from the h-GaN{000$\bar{2}$} plane was widely spread between the GaAs(3$\bar{3}$5)B and (335)B diffraction spots, and, as a consequence, that the films were no longer single-phase h-GaN but polycrystalline h-GaN. This result can be interpreted as follows. Different from on (11$\bar{n}$)B, two {335}B planes [(3$\bar{3}$5) and (3$\bar{3}$5)] have the same density on the (11n)A surfaces. Therefore, the h-GaN⟨0001⟩ direction, which tends to be parallel to the GaAs⟨335⟩B directions as shown, can not be determined uniquely, and many grains with different c-axis orientations between two GaAs ⟨335⟩B directions are formed. On the other hand, GaN on AlAs/GaAs(112)A or (111)A showed basically the same crystallographic properties as on GaAs(1$\bar{1}$2)B and (1$\bar{1}$1)B.

An interesting factor determining the crystallographic properties of GaN on AlAs/GaAs emerges from a comparison between the growth on the A and B substrates, which is the polarity. It is often reported that GaN grown on sapphire(0001) by MOVPE has cation (Ga) polarity (A polarity),[12] suggesting that it is MOVPE growth that causes GaN to have cation polarity because sapphire can not affect the GaN polarity due to its crystalline structure. In fact, it was confirmed that the surface morphology of our GaN grown directly on GaAs(111)A was much better than that of GaN on GaAs(1$\bar{1}$1)B, which supports that our growth conditions were suitable for cation-polar GaN, same as usual MOVPE. However, the pole figure measurements indicated that h-GaN{0001} plane always tends to be parallel to the anion-polar (i.e., B polar) GaAs{335} planes. From these findings, we consider that cation-polar GaN is grown on the anion-polar AlAs/GaAs plane. At present, it is supposed that AlAs inverts the polarity from A to B and vice versa during the nucleation of GaN on AlAs/GaAs. In order to confirm this hypothesis, an investigation on the polarity is in progress.

Note that all data shown are for the GaN on AlAs/GaAs{11n} grown at a low temperature (650 °C). The low-temperature growth is preferable for the nucleation of GaN on foreign substrates such as GaAs and sapphire, though the properties of low-temperature grown GaN are generally poorer than those of high-temperature grown GaN. Therefore, on thin (~50 nm) GaN grown at 650 °C on AlAs/GaAs(11$\bar{4}$)B, which exhibited the best crystallinity among those grown on the GaAs{11n} substrates, GaN 370 nm thick was grown at higher temperatures. Tentative (not optimized) growth conditions were a growth temperature of 850–950 °C, a V/III ratio of 25, and a growth rate of 1.1 μm h^{-1}. Figure 4 shows a low-temperature (9 K) photoluminescence (PL) spectrum of GaN grown at 950 °C. The dominant emission at 3.467 eV is probably due to donor bound excitons and its linewidth was as narrow as 14 meV. This emission is followed by a longitudinal optical-phonon replica, which appears as a small shoulder at around 3.37 eV. The weaker emission at 3.414 eV will be defect related, as reported by Fischer *et al.*[13] The temperature dependence of the emission at 3.285 eV suggested that this peak originates from the free-to-acceptor transition. Although the yellow band emission peaking at 2.27 eV is still strong, the PL properties were remarkably improved, compared with the PL properties of h-GaN grown on the AlAs/GaAs(001) substrate (see Fig. 4 in Ref. 7), and a further improvement is expected by increasing the film thickness and optimizing the growth conditions.

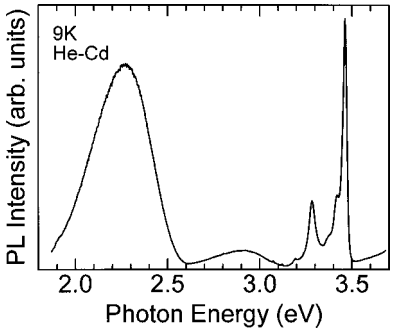

FIG. 4. Low-temperature (9 K) PL spectrum of GaN grown at 950 °C on AlAs/GaAs(11$\bar{4}$)B.

A part of the experiments was carried out at the Kyoto University Venture Business Laboratory (KU-VBL).

[1] S. Nakamura, S. Pearton, and G. Fasol, *Blue Laser Diode*, 2nd ed. (Springer, Heidelberg, 2000).
[2] A. Strittmatter, A. Krost, M. Straßburg, V. Trück, D. Bimberg, J. Bläsing, and J. Christen, Appl. Phys. Lett. **74**, 1242 (1999).
[3] A. Thamm, O. Brandt, Y. Takemura, A. Tranpert, and K. H. Ploog, Appl. Phys. Lett. **75**, 944 (1999).
[4] H. Okumura, S. Misawa, and S. Yoshida, Appl. Phys. Lett. **59**, 1058 (1991).
[5] M. Sasaki, T. Nakayama, N. Shimoyama, T. Suemasu, and F. Hasegawa, Jpn. J. Appl. Phys., Part 1 **39**, 4869 (2000).
[6] M. Ogawa, M. Funato, T. Ishido, S. Fujita, and S. Fujita, Jpn. J. Appl. Phys., Part 2 **39**, L69 (2000).
[7] M. Funato, T. Ishido, A. Hamaguchi, S. Fujita, and S. Fujita, Appl. Phys. Lett. **77**, 244 (2000).
[8] T. Ishido, M. Funato, A. Hamaguchi, S. Fujita, and S. Fujita, J. Cryst. Growth **221**, 280 (2000).
[9] A. Hamaguchi, M. Funato, T. Ishido, S. Fujita, and S. Fujita, *Proceedings of the International Workshop on Nitride Semiconductors, Nagoya, Japan, 24–27 September 2000*, IPAP Conference Series 1, (2000), p. 331.
[10] We define the substrate orientation as (11n) for A substrates and (11$\bar{n}$) for B substrates.
[11] For example, see K. Nakashima, J. Appl. Phys. **71**, 1189 (1992).
[12] E. S. Hellman, MRS Internet J. Nitride Semicond. Res. **3**, 11 (1998), and references therein.
[13] S. Fischer, G. Steude, D. M. Hofmann, F. Kurth, F. Anders, M. Topf, B. K. Meyer, F. Bertram, M. Schmidt, J. Christen, L. Eckey, J. Holst, A. Hoffmann, B. Mensching, and B. Rauschenbach, J. Cryst. Growth **189**, 556 (1998).